Proceeding of the IEEE
International Conference on Robotics and Biomimetics
Dali, China, December 2019

A Kinematic Equivalence Trajectory Planning Method of Hybrid Active and Passive Cable-Driven Segmented Hyper-Redundant Manipulator*

Zhonghua Hu, Taiwei Yang, Wenfu Xu*,
Zonggao Mu and Jianqing Peng
School of Mechanical Engineering and Automation
Harbin Institute of Technology, Shenzhen
Shenzhen, Guangdong Province, 518055, China
hitsz_hzh@163.com; taiweiyoung@outlook.com
wfxu@hit.edu.cn; muzonggao@163.com; pjqxs@163.com
Wenfu Xu is the corresponding author.

Bin Liang
Department of Automation
Tsinghua University
Beijing, 100000, *China*
bliang@mail.tsinghua.edu.cn

***Abstract* - A hybrid active and passive cable-driven segmented hyper-redundant manipulator is very flexible and dexterous to conduct tasks in highly cluttered environment. However, computation load of inverse kinematics and trajectory planning are also very large. In the paper, a kinematic equivalence method is proposed for the hybrid active and passive cable-driven segmented hyper-redundant manipulator to overcome the above challenge when the position and direction of end-effector are considered. The kinematic equivalence method is an effective way to solve the inverse kinematics and trajectory planning by simplifying and rearranging joints of each segment. The mechanism and joint layout of the manipulator are first analyzed. Then, the kinematics model is established by both traditional DH method and kinematic equivalence method. The calculated amount is decreased by reducing the number of rotation axis that needs to be processed in each segment. Furthermore, the desired trajectory is generated for the end effector of the arm to approach the target point. Finally, the proposed method is applied to a practical prototype, which has five segments and each segment consists of six subsegments. Simulation results verified the proposed method.**

Index Terms* - *Hyper-redundant manipulator; Hybrid active and passive cable-driven; kinematic equivalence; Trajectory planning.

I. INTRODUCTION

A hyper-redundant manipulator, which consists of a large number of degrees of freedom (DOFs), has more advantages for traditional robotic arms when performing some tasks in narrow and cluttered environment [1-5]. However, with the increase of DOFs, it will pose great challenges for the inverse kinematics and trajectory planning of hyper-redundant manipulator.

Recently, the scholars are committed to studying the related issues of motion planning of hyper-redundant manipulator. In order to deal with obstacle avoidance problem, G. S. Chirikjian [6] proposed a geometric algorithm which can determine an appropriate configuration on the planar hyper-redundant manipulator based on tunnel constraints. Samer et al [7] presented another geometrical method for the inverse kinematics of planar redundant manipulators. In the algorithm, the angles between the adjacent links are set to be equal to avoid singularity. Aime et al [8] developed a posture control approach which used the simple Jacobian formulation to achieve arbitrary posture tracking for hyper-redundant planar arms. Based on ant colony optimization (ACO), Zhao et al [9] presented a strategy which can be used to generate a number of random paths for the motion planning of a planar hyper-redundant manipulator. To explore the task space in R2, the Productive Regions Oriented Task (PROT) planner method [10] was proposed by Junghwan Lee for hyper-redundant manipulators. The researches results above focused exclusively the kinematics and trajectory planning of hyper-redundant arms in two dimensions space.

In addition to these algorithms, a few of methods have been introduced for motion planning of hyper-redundant arms in three dimensions space. G. S. Chirikjian [11] proposed a modal approach which was based on backbone curve to solve the inverse kinematics problem of hyper-redundant manipulators efficiently. According to the task requirement and working condition in space, Wenfu Xu [12] presented a modified modal method for solving the mission-oriented inverse kinematics. In the method, he used a mode function to define the spatial backbone of the hyper-redundant manipulator. Lukáš Bláha [13] developed a path planning method of hyper-redundant manipulator. The computational process was simplified by transforming robot joint space to developed view and back that was extremely useful for path planning and obstacle avoidance. Using the HyperBumpSurface concept to describe the 3D workspace,

*This work was supported by the National Key R&D Program of China (2018YFB1304600), National Natural Science Foundation of China (61903100), the Key Research and Development Program of Guangdong Province (2019B090915001), Guangdong Special Support Program (2017TX04X0071) and the Basic Research Program of Shenzhen (JCYJ20180507183610564), the National Postdoctoral Program for Innovative Talents (Grant No. BX20180089) and China Postdoctoral Science Foundation (Grant No. 2018M641817).

978-1-7281-6321-5/19//$31.00 ©2019 IEEE

Elias K. Xidias [14] proposed a time-optimal trajectory planning method which can move the hyper-redundant manipulator from an initial configuration to a final configuration. On the basis of iterative approach, another efficient algorithm was presented by Liangliang Zhao [15] to solve the inverse solutions of hyper-redundant manipulators and to avoid the moving obstacles. Taking a hyper-redundant manipulator as the human arm, the hyper-redundant manipulator can be segmented into three sections, i.e., shoulder, elbow, and wrist. And Zonggao Mu et al [16] proposed a segmented geometry method to solve the inverse solutions and to control the configuration for spatial hyper-redundant manipulators. Based on the cyclic coordinate descent (CCD) algorithm, Andrés [17] presented a new method to obtain the best solution. In addition, the method was also helpful for continuous trajectories performance and motion planning analysis in highly constrained environments. For previous works, the whole joints of manipulators that the scholars proposed are active. But for the manipulators we designed, its joints are the hybrid active and passive.

In fact, the hybrid active and passive joints, used in the hyper-redundant arm will bring great challenges to inverse kinematics or trajectory planning in three dimensions space. Hence, we present a kinematic equivalence method to solve the above issues. The innovation and advantages of the work is that the computation load of trajectory planning is reduced largely. This paper is organized as follows: Section II analyzes mechanism and the joint layout of the proposed manipulator and derives the kinematics equations by traditional DH method. Section III defines the kinematic equivalence and gives kinematics equations based on kinematic equivalence method. Then, a trajectory planning method is addressed to track the desired point in Section IV. In Section V, a simulation is developed to verify it is of high precision for the cable-driven segmented hyper-redundant manipulator to trace a spatial arc based on kinematic equivalence method. Finally, the conclusions and discussions are presented in Section VI.

II. Kinematics of the Cable-Driven Segmented Hyper-Redundant Manipulator

A. Analysis of the Mechanism

The cable-driven segmented hyper-redundant manipulator is composed of N segments. For each segment, there are n subsegments and each subsegment contains a universal joint and a rigid link attached to the former. Where, symbol N and n are integers that are greater than or equal to 2. Moreover, one of the segments has the identical mechanical structure similar to that of any other segments. The general model of the cable-driven segmented hyper-redundant manipulator is shown in Fig. 1.

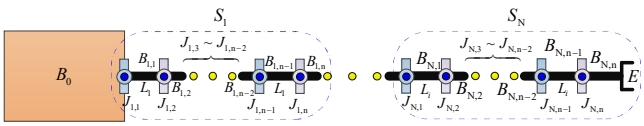

Fig. 1 General model of the developed hyper-redundant Manipulator

Here, the meaning of each symbol is given as followed. The symbol B_0 represents the base of the developed manipulator. The symbol S_i is the i^{th} segment and $B_{i,j}$ is the j^{th} subsegment of S_i. The length of the rigid link in the $B_{i,j}$ can be denoted by L_i. And the symbol $J_{i,j}$ represents j^{th} universal joint which is used to connected the (j-1)th subsegment and j^{th} subsegment in the S_i. The symbol E is the end-effector of the cable-driven segmented hyper-redundant manipulator.

B. Joint Layout of the Proposed Manipulator

As shown in Fig. 1, each segment of the developed manipulator has the identical joint layout because of the same mechanical structure. So, taking the first segment for example, its joint layout is shown in Fig. 2 in detail.

As is shown in the Fig. 2-(a), if n is even number, the structure of first segment is (Pitch-Yaw-Yaw-Pitch)…(Pitch-Yaw-Yaw-Pitch)-(Pitch-Yaw-Yaw-Pitch). On the other hand, the first segment is with the structure of (Pitch-Yaw-Yaw-Pitch)…(Pitch-Yaw-Yaw-Pitch)-(Pitch-Yaw), when n is odd number. Where, the symbol Σ_I represents the inertial coordinate system. Its coordinate axes are X_I, Y_I, and Z_I. The symbol $\theta_{i,j,k}$ represents the k^{th} rotation axis of the j^{th} universal joint in the i^{th} segment. The value of k is "1" or "2", because there are only two revolving axes in a universal joint. Therefore, the number "1" means the first rotation axis and "2" refers to the second rotation axis. Since the universal joints of each segment are hybrid active and passive, i.e. the first universal joint is active joint which can be controlled according to demand and the rest universal joints are passive joints that will move with the first universal joint at the identical angle in the same direction. Furthermore, the motion laws of all universal joints can be expressed as followed.

$$\begin{cases} \theta_{i,j,1} = \theta_{i,j+1,2} \\ \theta_{i,j,2} = \theta_{i,j+1,1} \end{cases} \quad i = 1,2,\ldots,N;\ j = 1,2,\ldots,n-1 \qquad (1)$$

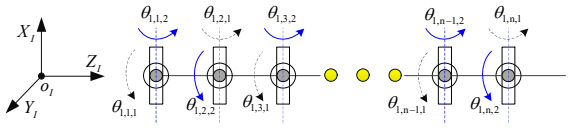

(a) n is even number

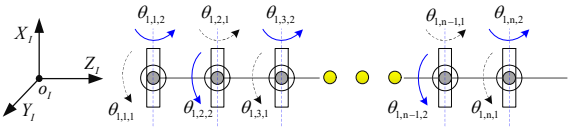

(b) n is odd number

Fig. 2 The joint layout of the first segment

C. Kinematics Analysis with Traditional Method

It can be known from Section II.A that each segment has n universal joints. And there are two orthogonal revolving axes for every universal joint. Hence each segment has 2*n revolving axes which are N*(2*n) for the manipulator we proposed. According to the classical D-H method, D-H frames can be established for each rotation axis. Then the first segment has 2*n groups D-H parameters. Therefore, that are

N*(2*n) for the whole manipulator. By using of the D-H parameters, the homogeneous transformation matrix from the end of cable-driven segmented hyper-redundant manipulator to the reference frame can be obtained as follows:

$$ {}^{0}\boldsymbol{T}_{e} = \prod_{i=1}^{N}\prod_{j=1}^{n}\left(\boldsymbol{T}_{i,j,1}\cdot\boldsymbol{T}_{i,j,2}\right) \tag{2} $$

where,

$$ \boldsymbol{T}_{i,j,k} = \begin{bmatrix} c_{\theta_{i,j,k}} & -s_{\theta_{i,j,k}}c_{\alpha_{i,j,k}} & s_{\theta_{i,j,k}}s_{\alpha_{i,j,k}} & a_{i,j,k}c_{\theta_{i,j,k}} \\ s_{\theta_{i,j,k}} & c_{\theta_{i,j,k}}c_{\alpha_{i,j,k}} & -c_{\theta_{i,j,k}}s_{\alpha_{i,j,k}} & a_{i,j,k}s_{\theta_{i,j,k}} \\ 0 & s_{\alpha_{i,j,k}} & c_{\alpha_{i,j,k}} & d_{i,j,k} \\ 0 & 0 & 0 & 1 \end{bmatrix} \tag{3} $$

So, the amount of computation of the traditional D-H method is 2**N***n* operations of the 4 by 4 matrix multiplication in order to obtain the pose of the end-effector.

III. The Kinematic Equivalence Method for the Developed Manipulator

A. The Concept of Kinematic Equivalence method

The cable-driven segmented hyper-redundant manipulator has more flexibility and dexterity for complicated operation tasks, such as pipeline detection, rescue after disaster and nuclear plant maintenance. So trajectory planning plays an important role for the cable-driven segmented hyper-redundant manipulator to complete these tasks. However, the position and direction vector of the end-effector are only taken into consideration in most cases. As for this, the kinematic equivalence method is proposed for the hyper-redundant manipulator. Kinematic equivalence means that the kinematics model (position and direction vector of the end of any segment) of a new hyper-redundant manipulator which is be constructed by simplifying and rearranging joints in each segment is equivalent to that of the developed hyper-redundant manipulator shown in Fig. 1.

Similar to the original hyper-redundant manipulator, each segment of the kinematic equivalence hyper-redundant manipulator is also consist of the same joint layout. Hence, taking the first segment of kinematic equivalence hyper-redundant manipulator for instance, the specific joint layout only is (Roll-Yaw)-Yaw-Yaw…Yaw-Yaw that is shown in Fig. 3, whether *n* is even number or odd number. Furthermore, there are also *n* joints for each segment of the kinematic equivalence hyper-redundant manipulator. And the first is universal joint which is active joint and is formed by Roll axis and Yaw axis. The others are revolving joints that are passive joint rotating in the direction of Yaw axis. The rotation angle of each passive joint is equal to that of the Yaw axis of the first joint, i.e.,

$$ \alpha_{1,1} = \alpha_{1,2} = \alpha_{1,3} = \ldots = \alpha_{1,n-1} = \alpha_{1,n} \tag{4} $$

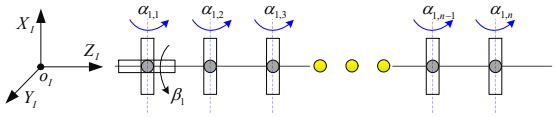

Fig. 3 The joint layout of the first segment for the equivalence manipulator

B. Kinematics Analysis with Kinematic Equivalence Method

As shown in Fig. 3, there are *n*+1 rotation axes for each segment of the kinematic equivalence hyper-redundant manipulator. For the i^{th} segment, the movement angle of the first rotation axis can be denoted by β_i. And the symbol α_i is the rotation angle of the second rotation axis. In addition, the movement angles of the others which are moving with the second rotation axis synchronously can be also written as α_i. Hence, the homogeneous transformation matrix from the end of i^{th} segment to the end of (i-1)th segment can be expressed as

$$ \begin{aligned} \boldsymbol{T}_i &= Rot\left(z,\beta_i\right)\cdot\prod_{j=1}^{n}\left(Rot\left(x,\alpha_i\right)\cdot Trans\left(z,L_i\right)\right) \\ &= \begin{bmatrix} c_{\beta_i} & -s_{\beta_i}c_{n\alpha_i} & s_{\beta_i}s_{n\alpha_i} & s_{\beta_i}\sum_{j=1}^{n}s_{j\alpha_i}L_i \\ s_{\beta_i} & c_{\beta_i}c_{n\alpha_i} & c_{\beta_i}s_{n\alpha_i} & -c_{\beta_i}\sum_{j=1}^{n}s_{j\alpha_i}L_i \\ 0 & s_{n\alpha_i} & c_{n\alpha_i} & \sum_{j=1}^{n}c_{j\alpha_i}L_i \\ 0 & 0 & 0 & 1 \end{bmatrix} = \begin{bmatrix} & \boldsymbol{R}_i & & \boldsymbol{p}_i \\ [0 & 0 & 0] & 1 \end{bmatrix} \end{aligned} \tag{5} $$

According to (5), the pose of the end-effector of the kinematic equivalence hyper-redundant manipulator is yielded by recursion law, i.e.,

$$ \begin{aligned} \boldsymbol{T}_E &= \boldsymbol{T}_1\cdot\boldsymbol{T}_2\cdot\boldsymbol{T}_3\cdot\ldots\cdot\boldsymbol{T}_{N-1}\cdot\boldsymbol{T}_N = \prod_{i=1}^{N}\boldsymbol{T}_i \\ &= \begin{bmatrix} \prod_{i=1}^{N}\boldsymbol{R}_i & \boldsymbol{p}_1 + \sum_{i=2}^{N}\left(\left(\prod_{j=1}^{i-1}\boldsymbol{R}_j\right)\cdot\boldsymbol{p}_i\right) \\ \boldsymbol{0}_{1\times3} & 1 \end{bmatrix} = \begin{bmatrix} \boldsymbol{R}_E & \boldsymbol{p}_E \\ \boldsymbol{0}_{1\times3} & 1 \end{bmatrix} \end{aligned} \tag{6} $$

In conclusion, the proposed method needs only 2**N* operations of the 4 by 4 matrix multiplication which is far less than that of traditional D-H method (2*N**n* operations). The linear and angular velocities of the end effector of the kinematic equivalence hyper-redundant manipulator can be solved by differentiating (6), when $\boldsymbol{T}_E$ is determined. First, the angular velocity of the end effector can be obtained as shown in (7).

$$ \begin{aligned} \boldsymbol{\omega}_E^{\times} &= \left(\frac{d}{dt}\prod_{i=1}^{N}\boldsymbol{R}_i\right)\cdot\left(\prod_{i=1}^{N}\boldsymbol{R}_i\right)^{\mathrm{T}} \\ &= \sum_{j=1}^{N}\left(\left(\frac{\partial}{\partial\beta_j}\prod_{i=1}^{N}\boldsymbol{R}_i\right)\dot{\beta}_i + \left(\frac{\partial}{\partial\alpha_j}\prod_{i=1}^{N}\boldsymbol{R}_i\right)\dot{\alpha}_j\right)\cdot\left(\prod_{i=1}^{N}\boldsymbol{R}_i\right)^{\mathrm{T}} \\ &= \sum_{j=1}^{N}\left(\boldsymbol{J}_{\omega\_\beta_j}^{\times}\cdot\dot{\beta}_j + \boldsymbol{J}_{\omega\_\alpha_j}^{\times}\cdot\dot{\alpha}_j\right) \end{aligned} \tag{7} $$

$$\begin{cases} \boldsymbol{J}^{\times}_{\omega\_\beta_j} = \left(\dfrac{\partial}{\partial \beta_j} \prod_{i=1}^{N} \boldsymbol{R}_i \right) \cdot \left(\prod_{i=1}^{N} \boldsymbol{R}_i \right)^{\mathrm{T}} \\ \boldsymbol{J}^{\times}_{\omega\_\alpha_j} = \left(\dfrac{\partial}{\partial \alpha_j} \prod_{i=1}^{N} \boldsymbol{R}_i \right) \cdot \left(\prod_{i=1}^{N} \boldsymbol{R}_i \right)^{\mathrm{T}} \end{cases} \tag{8}$$

$\boldsymbol{J}_{\omega\_\beta_j}$ and $\boldsymbol{J}_{\omega\_\alpha_j}$ are 3×1 vector and are obtained on the basis of (8). Furthermore, they are the Jacobian matrix that are related to angular velocity for the kinematic equivalence hyper-redundant manipulator.

Then the linear velocity of the end effector is solved by differentiating $\boldsymbol{p}_E$ in (6).

$$\begin{aligned} \boldsymbol{v}_E &= \frac{d}{dt}\left(\boldsymbol{p}_1 + \sum_{i=2}^{N} \left(\left(\prod_{j=1}^{i-1} \boldsymbol{R}_j \right) \cdot \boldsymbol{p}_i \right) \right) \\ &= \sum_{j=1}^{N} \left(\frac{\partial \boldsymbol{p}_e}{\partial \beta_j} \cdot \dot{\beta}_j + \frac{\partial \boldsymbol{p}_e}{\partial \alpha_j} \cdot \dot{\alpha}_j \right) \\ &= \sum_{j=1}^{N} \left[\boldsymbol{J}_{v\_\beta_j} \quad \boldsymbol{J}_{v\_\alpha_j} \right] \cdot \begin{bmatrix} \dot{\beta}_j \\ \dot{\alpha}_j \end{bmatrix} \end{aligned} \tag{9}$$

$$\begin{cases} \boldsymbol{J}_{v\_\beta_j} = \dfrac{\partial}{\partial \beta_j} \left(\boldsymbol{p}_1 + \sum_{i=2}^{N} \left(\left(\prod_{k=1}^{i-1} \boldsymbol{R}_k \right) \cdot \boldsymbol{p}_i \right) \right) \\ \boldsymbol{J}_{v\_\alpha_j} = \dfrac{\partial}{\partial \alpha_j} \left(\boldsymbol{p}_1 + \sum_{i=2}^{N} \left(\left(\prod_{k=1}^{i-1} \boldsymbol{R}_k \right) \cdot \boldsymbol{p}_i \right) \right) \end{cases} \tag{10}$$

$\boldsymbol{J}_{v\_\beta_j}$ and $\boldsymbol{J}_{v\_\alpha_j}$ are 3×1 vector and are obtained according to (10). Moreover, they are the Jacobian matrix connection with linear velocity for the kinematic equivalence hyper-redundant manipulator.

Combining (8) and (10), the Jacobian matrix of the kinematic equivalence hyper-redundant manipulator is determined as follows

$$\boldsymbol{J}_{Eq} = \begin{bmatrix} \boldsymbol{J}_{v\_\beta_1}, & \boldsymbol{J}_{v\_\alpha_1}, & \boldsymbol{J}_{v\_\beta_2}, & \boldsymbol{J}_{v\_\alpha_2} & \cdots & \boldsymbol{J}_{v\_\beta_N} & \boldsymbol{J}_{v\_\alpha_N} \\ \boldsymbol{J}_{\omega\_\beta_1}, & \boldsymbol{J}_{\omega\_\alpha_1}, & \boldsymbol{J}_{\omega\_\beta_2}, & \boldsymbol{J}_{\omega\_\alpha_2} & \cdots & \boldsymbol{J}_{\omega\_\beta_N} & \boldsymbol{J}_{\omega\_\alpha_N} \end{bmatrix} \tag{11}$$

Hence, the linear and angular velocities of the end effector is derived as follows

$$\begin{bmatrix} \boldsymbol{v}_E \\ \boldsymbol{\omega}_E \end{bmatrix} = \boldsymbol{J}_{Eq} \dot{\boldsymbol{\Theta}}_{Eq} \tag{12}$$

where $\dot{\boldsymbol{\Theta}}_{Eq}$ is 2N×1 vector that is consist of the joint rate of the kinematic equivalence hyper-redundant manipulator.

IV. Trajectory Planning with the Kinematic Equivalence Method

A. Trajectory planning of the end effector after kinematic equivalence

The desired linear velocity and angular velocity of the end effector of the kinematic equivalence arm are obtained as followed

$$\begin{bmatrix} \boldsymbol{v}_{ed} \\ \boldsymbol{\omega}_{ed} \end{bmatrix} = \boldsymbol{K}_p \begin{bmatrix} \Delta \boldsymbol{p}_e \\ \Delta \boldsymbol{O}_e \end{bmatrix} \tag{13}$$

where $\boldsymbol{K}_p$ is the proportion coefficient matrix. $\Delta \boldsymbol{p}_e$ and $\Delta \boldsymbol{O}_e$ are the position and orientation deviations between the end effector of the kinematic equivalence arm and the desired point respectively.

In the paper, we will only focus on Z-axis direction deviation between the end effector of the kinematic equivalence arm and the desired point. Hence, $\Delta \boldsymbol{p}_e$ and $\Delta \boldsymbol{O}_e$ are given by

$$\Delta \boldsymbol{p}_e = \boldsymbol{p}_t - \boldsymbol{p}_e \tag{14}$$

$$\Delta \boldsymbol{O}_e = \frac{\boldsymbol{a}_e \times \boldsymbol{a}_t}{\left\| \boldsymbol{a}_e \times \boldsymbol{a}_t \right\|} \phi \tag{15}$$

where $\boldsymbol{p}_t$ and $\boldsymbol{a}_t$ are the position and direction vectors of the desired point and $\boldsymbol{p}_e$ and $\boldsymbol{a}_e$ are the position and direction vectors of the end effector of the kinematic equivalence arm respectively. ϕ is the angle between the vectors $\boldsymbol{a}_t$ and $\boldsymbol{a}_e$. It can be solved as followed

$$\phi = \arccos(\boldsymbol{a}_e^{\mathrm{T}} \cdot \boldsymbol{a}_t) \tag{16}$$

B. Resolved joint motion for the kinematic equivalence arm

Combining (12) and (13), the desired velocities of the end effector are given by

$$\begin{bmatrix} \boldsymbol{v}_{ed} \\ \boldsymbol{\omega}_{ed} \end{bmatrix} = \boldsymbol{K}_p \begin{bmatrix} \Delta \boldsymbol{p}_e \\ \Delta \boldsymbol{O}_e \end{bmatrix} = \boldsymbol{J}_{Eq} \dot{\boldsymbol{\Theta}}_{Eq} \tag{17}$$

Therefore, desired joint rates of the kinematic equivalence arm can be resolved as follows

$$\dot{\boldsymbol{\Theta}}_{Eq} = \left(\boldsymbol{J}_{Eq} \right)^{-1} \left(\boldsymbol{K}_p \begin{bmatrix} \Delta \boldsymbol{p}_e \\ \Delta \boldsymbol{O}_e \end{bmatrix} \right) \tag{18}$$

According to (18), $\boldsymbol{J}_{Eq}$ is not square matrix and $(\boldsymbol{J}_{Eq})^{-1}$ is pseudo-inverse of the matrix $\boldsymbol{J}_{Eq}$, when the number N is not equal to 3. Then, the desired joint angles can be calculated by the numerical integration, such as

$$\boldsymbol{\Theta}_{Eq}(t + \Delta t) = \boldsymbol{\Theta}_{Eq}(t) + \dot{\boldsymbol{\Theta}}_{Eq}(t) \Delta t \tag{19}$$

C. Calculated joint angles of the original hyper-redundant manipulator

In practical application, the joint angles are the key to the original hyper-redundant manipulator for completing the complicated tasks. These angles can be obtained when joint angles of the kinematic equivalence arm are known. Hence, taking the first segment for example, the calculation process of joint angles of the original equivalence is given as followed.

It is well known that all the subsegments of the first segment are in the same plane. Furthermore, the angles of any two adjacent subsegments are equal.

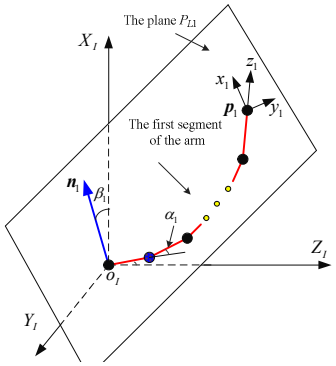

Fig. 4 The first segment of the hyper-redundant manipulator

As shown in Fig. 4, the first segment of the hyper-redundant manipulator is in the plane P_{L1}. And $\boldsymbol{n}_1$ is the normal vector of the plane P_{L1}. For the kinematic equivalence arm, $\boldsymbol{n}_1$ projected in the inertial frame is obtained as followed

$$\boldsymbol{n}_1 = \boldsymbol{x}_1 = \left[\boldsymbol{T}_1(1,1) \quad \boldsymbol{T}_1(2,1) \quad \boldsymbol{T}_1(3,1)\right]^{\mathrm{T}} = \left[c_{\beta_i} \quad s_{\beta_i} \quad 0\right]^{\mathrm{T}} \tag{20}$$

The symbol Σ_1 represents the coordinate system fixed on the end of the first segment of the kinematic equivalence arm. And $\boldsymbol{x}_1$ is the x-axis of the Σ_1. $\boldsymbol{T}_1$ is the homogeneous transformation matrix from the end of the first segment to the installation location of the manipulator and is calculated by (5). And $\boldsymbol{T}_1(i, j)$ is element in the row i, column j of $\boldsymbol{T}_1$.

The cosines for the angles of any two adjacent subsegments is yielded by

$$\Gamma_1 = c_{\alpha_1} \tag{21}$$

On the one hand, $\boldsymbol{n}_1$ and the cosines for the angles of any two adjacent subsegments can be also obtained for the original hyper-redundant manipulator.

$$\boldsymbol{n}_1 = \frac{\left[s_{\theta_{12}} \quad s_{\theta_{11}} c_{\theta_{12}} \quad 0\right]^{\mathrm{T}}}{\sqrt{1-\left(c_{\theta_{11}} c_{\theta_{12}}\right)^2}} \tag{22}$$

$$\Gamma_1 = c_{\theta_{11}} c_{\theta_{12}} \tag{23}$$

Combining (21), (22), and (23), the joint angles of first segment of the original manipulator can be solved when the β_1 and α_1 are known.

$$\begin{cases} \theta_{11} = \operatorname{atan2}\left(s_{\beta_i} \cdot \sqrt{1-c_{\alpha_1}{}^2}, c_{\alpha_1}\right) \\ \theta_{12} = \arcsin\left(c_{\beta_i} \cdot \sqrt{1-c_{\alpha_1}{}^2}\right) \end{cases} \tag{24}$$

The rest of the joint angles of the original arm can be solved by the same way.

V. Simulation Study

A. Simulation modeling of the spatial arc and the manipulator

To validate the validity of the method, a spatial arc is designed for the hyper-redundant manipulator to trace. A spatial arc is determined by the center $\boldsymbol{O}_c(x_c, y_c, z_c)$, radius vector $\boldsymbol{R}_0$ that is the position vector from the center to the initial point of the spatial arc, and the normal vector $\boldsymbol{n}_c$ of the plane that the spatial arc is in. Therefore, for any point in the spatial arc, its position vector in the inertial frame are obtained as followed

$$\boldsymbol{P}_c = \boldsymbol{O}_c + e^{\eta \cdot \boldsymbol{n}_c^{\times}} \cdot \boldsymbol{R}_0 \tag{25}$$

$$e^{\eta \cdot \boldsymbol{n}_c^{\times}} = \boldsymbol{I} + \sin(\eta) \cdot \boldsymbol{n}_c^{\times} + \left(1-\cos(\eta)\right) \cdot \boldsymbol{n}_c^{\times} \cdot \boldsymbol{n}_c^{\times} \tag{26}$$

where η is the central angle and $\boldsymbol{I}$ is 3×3 unit matrix.

Then, the hybrid active and passive cable-driven segmented hyper-redundant manipulator, shown in Fig. 5, is taken as the example for simulation study. The manipulator is composed of a base and 5 segments, each of which has 6 subsegments with the same structures. The length of the rigid link in each subsegment is 0.1 m, where $X_IY_IZ_I$ is the inertia frame.

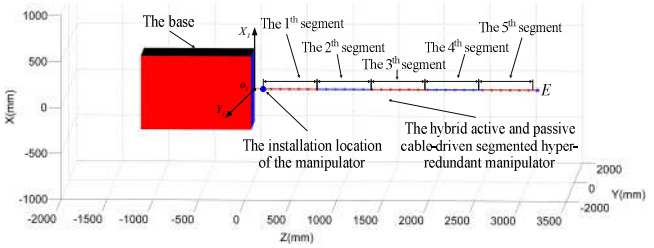

Fig. 5 The model of the cable-driven segmented hyper-redundant manipulator

B. Trajectory tracking simulation

In this section, the hybrid active and passive cable-driven segmented hyper-redundant manipulator are used to trace a spatial arc. The parameters of the spatial arc are as follows

$$\begin{cases} \boldsymbol{O}_c = \left[0.35\text{m} \quad -0.05\text{m} \quad 1.45\text{m}\right]^{\mathrm{T}}, \boldsymbol{n}_c = \left[0 \quad 0 \quad 1\right]^{\mathrm{T}} \\ \boldsymbol{R}_0 = \left[0\text{m} \quad 0.3\text{m} \quad 0\text{m}\right]^{\mathrm{T}}, \eta \in [0^\circ, \ 100^\circ] \end{cases} \tag{27}$$

The boundary conditions of each joint angle for the original hyper-redundant manipulator are as follows

$$\begin{cases} -15^\circ \le \theta_{i,j,1} \le 15^\circ \\ -15^\circ \le \theta_{i,j,2} \le 15^\circ \end{cases}, \quad i = 1,2,4,5 \text{ and } j = 1,2,4,5,6 \tag{28}$$

Hence the boundary conditions of each joint angle for the kinematic equivalence arm are as follows

$$\begin{cases} -180^\circ \le \beta_i \le 180^\circ \\ 0^\circ \le \alpha_i \le \arccos\left(\cos^2\left(15^\circ\right)\right) \end{cases} \quad i = 1,2,4,5 \tag{29}$$

Then, the kinematic equivalence method is simulated by using MATLAB software. In the simulation, the spatial arc is divided equally into 100 segment with 101 nodes. And we assume that it will take 0.1 second to obtain the joints' angle data for the manipulator to actuate the end-effector from current node to next node. According to the simulation results, the curves of relative position and direction deviations between the end effector and the desired node in spatial arc are shown in Fig. 6.

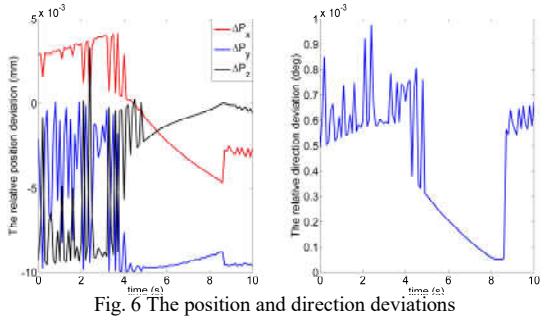

Fig. 6 The position and direction deviations

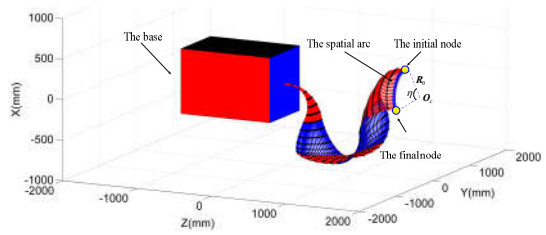

Fig. 7 The variation of the configuration

In the simulation, the position deviation is smaller than 0.01 mm and the direction deviation is smaller than 0.001° at various moments. It means that the desired node can be traced with high accuracy for the end effector by using the kinematic equivalence method. Configurations of the 3D model at different times during the simulation are shown in Fig. 7.

VI. Conclusion

The research about trajectory planning of hybrid active and passive cable-driven segmented hyper-redundant manipulator was difficult because of its vast DOFs and complicated mechanism. In the face of these difficulties, the kinematic equivalence method is proposed in the paper. First of all, the kinematic is modeled by using of the traditional DH method and the kinematic equivalence method. And it can be concluded that the amount of computation of the kinematic equivalence method is smaller than that of DH method. Then, the trajectory planning based on kinematic equivalence method is designed for the hyper-redundant manipulator. Finally, a simulation system for the manipulator tracing a spatial arc is established. The simulation results show that the arm can approach the desired point on the spatial arc with high precision based on the proposed method.

Another issue which is worth studying is to realize the optimization of configurations for the hybrid active and passive cable-driven segmented hyper-redundant manipulator by the kinematic equivalence method. In the future, we will carry out this research.

References

[1] G. S. Chirikjian and J. W. Burdick, "A hyper-redundant manipulator," *IEEE Robotics & Automation Magazine*, vol. 1, no. 4, pp. 22-29, 1994.

[2] G. S. Chirikjian and J. W. Burdick, "An obstacle avoidance algorithm for hyper-redundant manipulators," *in IEEE International Conference on Robotics and Automation*, Cincinnati, USA, 1990, pp. 625-631.

[3] W. Xu, T. Liu and Y. Li, "Kinematics, Dynamics, and Control of a Cable-Driven Hyper-Redundant Manipulator," *IEEE/ASME Transactions on Mechatronics*, vol. 23, no. 4, pp. 1693-1704, 2018.

[4] Y. B., H. L., L. G., X. W., and H. B., "A modular amphibious snake-like robot: Design, modeling and simulation," *in IEEE International Conference on Robotics and Biomimetics (ROBIO)*, Zhuhai, China, 2015, pp. 1924-1929.

[5] H. S., Z. Q., L. Z., W. X., and L. B., "Control of a piecewise constant curvature continuum manipulator via policy search method," *in IEEE International Conference on Robotics and Biomimetics (ROBIO)*, Kuala Lumpur, Malaysia, 2018, pp. 1777-1782.

[6] G. S. Chirikjian and J. W. Burdick, "A Geometric Approach to Hyper-Redundant Manipulator Obstacle Avoidance," *Journal of Mechanical Design*, vol. 114, no. 4, pp. 580-585, 1992.

[7] S. Yahya, M. Moghavvemi and H. A. F. Mohamed, "Geometrical approach of planar hyper-redundant manipulators: Inverse kinematics, path planning and workspace," *Simulation Modelling Practice and Theory*, vol. 19, no. 1, pp. 406-422, 2011.

[8] A. C. A. Dione, S. Hasegawa and H. Mitake, "Stable posture control for planar hyper-redundant arms using selective control points," *Advanced Robotics*, vol. 31, no. 23-24, pp. 1338-1348, 2017.

[9] Z. J., Z. L. and L. H., "Motion planning of hyper-redundant manipulators based on ant colony optimization," *in IEEE International Conference on Robotics and Biomimetics (ROBIO)*, Qingdao, China, 2016, pp. 1250-1255.

[10] L. J. and Y. S., "PROT: Productive regions oriented task space path planning for hyper-redundant manipulators," *in IEEE International Conference on Robotics and Automation (ICRA)*, Hong Kong, China, 2014, pp. 6491-6498.

[11] S. C. G. and W. B. J., "A modal approach to hyper-redundant manipulator kinematics," *IEEE Transactions on Robotics and Automation*, vol. 10, no. 3, pp. 343-354, 1994.

[12] W. Xu, Z. Mu, T. Liu, and B. Liang, "A modified modal method for solving the mission-oriented inverse kinematics of hyper-redundant space manipulators for on-orbit servicing," *Acta Astronautica*, vol. 139, pp. 54-66, 2017.

[13] B. L. and S. M., "Path planning of hyper-redundant manipulator in developed view," *in International Carpathian Control Conference (ICCC)*, Szilvasvarad, Hungary, 2018, pp. 295-300.

[14] E. Xidias, "Time-optimal trajectory planning for hyper-redundant manipulators in 3D workspaces," *Robotics and Computer-Integrated Manufacturing*, vol. 50, pp. 286-298, 2017.

[15] Z. L., Z. J., L. H., and M. D., "Efficient Inverse Kinematics for Redundant Manipulators with Collision Avoidance in Dynamic Scenes," *in IEEE International Conference on Robotics and Biomimetics (ROBIO)*, Kuala Lumpur, Malaysia, 2018, pp. 2502-2507.

[16] M. Z., Y. H., X. W., L. T., and L. B., "A Segmented Geometry Method for Kinematics and Configuration Planning of Spatial Hyper-Redundant Manipulators," *IEEE Transactions on Systems, Man, and Cybernetics: Systems*, vol. 99, pp. 1-11, 2018.

[17] A. Martín, A. Barrientos and J. Del Cerro, "The Natural-CCD Algorithm, a Novel Method to Solve the Inverse Kinematics of Hyper-redundant and Soft Robots," *Soft robotics*, vol. 5, no. 3, pp. 242-257, 2018.